Martin-Puplett interferometer: an analysis

D. K. Lambert and P. L. Richards

A detailed analysis is presented of the Michelson polarizing interferometer suggested by Martin and Puplett. This instrument has many favorable properties for use as a far ir Fourier spectrometer. The effect of misalignments and imperfections of the optical components on the instrumental performance is calculated. Based on these results, we give a method of aligning the interferometer which optimizes its performance. In addition, this instrument may be used to measure the optical transfer function of a component in the output beam as a function of both spatial and optical frequency. A procedure is described by which this may be done.

I. Introduction

As first pointed out by Martin and Puplett,[1] a version of the Michelson interferometer which uses a wire grid polarizer as a beam splitter and roof mirrors for reflectors has many advantages for far ir Fourier spectroscopy. This instrument is related to previous interferometers which make use of roof mirrors.[2,3] Over the past several years we have used the MPI (Michelson polarizing or Martin-Puplett interferometer) for laboratory and astrophysical[4] spectroscopy. The alignment procedure required to obtain ideal performance from this interferometer is not obvious at first sight.

In this paper we develop a mathematical description of the MPI. We make use of a theory described in more detail elsewhere[5] to compute the effects of all misalignments and imperfections of the optical components on instrumental performance. We then describe an alignment procedure which yields nearly ideal performance in practice.

In addition to its use as a Fourier spectrometer, one may also use the MPI as a shearing interferometer to measure the optical transfer function[6] (OTF) of an optical component located in the output beam. Our method of measuring the OTF is similar to a method used by Steel[7] with a visible polarizing interferometer. The method has the advantage that the measurement process itself gives the dependence of the OTF on optical frequency without further effort. It is different from other commonly used methods[8,9] in that it uses incoherent as opposed to coherent light.

The authors are with University of California, Department of Physics & Materials and Molecular Research Division, Lawrence Berkeley Laboratory, Berkeley, California 94720.

Received 13 August 1977.
0003-6935/78/0515-1595$0.50/0.

We begin our analysis by developing a vector notation to describe a perfectly aligned MPI. Although the discussion can be easily generalized to any of a number of essentially equivalent interferometers, we will refer specifically to the version shown in Fig. 1 which has been used in our laboratory. We describe the free standing wire grid beam splitter B by the unit vector $\hat{n}_B$ normal to the plane of the wires, the unit vector $\hat{u}_B$ perpendicular both to the wires and $\hat{n}_B$, and a point $\mathbf{x}_B$ in the plane of the wires. The roof mirrors R_1 and R_2 are described by the direction $\hat{n}_R$ along which the two mirrors forming the roof intersect, a point $\mathbf{x}_R$ along the line of intersection, and the actual dihedral angle θ_R between the two mirrors. A more complete specification of the roof mirrors will be discussed in the Appendix. The polarizers P_1 and P_2 are specified by the direction $\hat{u}$ of the electric field in light transmitted along the optic axis. One of these polarizers (P_2 in our case) is rotated with angular frequency ω so as to modulate the output of the interferometer at frequency 2ω. If we choose x and y axes as shown in Fig. 1 and a z axis directed up out of the plane, the instrument is perfectly aligned when $\hat{n}_B = [(1/\sqrt{2}), (1/\sqrt{2}), 0]$, $\hat{u}_B = (0,0,1)$, $\mathbf{x}_B = (0,0,0)$, $\hat{n}_{R1} = [0, -(1/\sqrt{2}), (1/\sqrt{2})]$, $\hat{n}_{R2} = [(1/\sqrt{2}), 0, (1/\sqrt{2})]$, $\mathbf{x}_{R1} = (-x_1,0,0)$, $\mathbf{x}_{R2} = (0,x_2,0)$, $\theta_{R1} = \theta_{R2} = \pi/2$, $\hat{u}_1 = [-(1/\sqrt{2}), 0, (1/\sqrt{2})]$, and $\hat{u}_2 = (0, \sin\omega t, \cos\omega t)$.

There is a useful geometric picture of the relationships among R_1, R_2, and B which helps to clarify the operation of the interferometer.[10] We imagine looking along the $-\hat{x}$ direction toward B so that we can see R_1 through it. We will also see the image of R_2 reflected in B. When the ideal instrument is adjusted to zero path difference, $x_1 = x_2$, we see the real image of the line of intersection of the mirrors of R_2 superposed on the line of intersection of the mirrors of R_1. There are four types of deviations from this superposed condition that can occur. The first, shown in Fig. 2(a), is the translation of one line relative to the other along the $\hat{x}$ axis.

This corresponds to a change of the optical path difference $x_1 - x_2$ between the two beams. The second, shown in Fig. 2(b), is a rotation of one line relative to the other in a plane containing the $\hat{x}$ axis. We call the angle θ_T between the two lines the angle of tilt. It corresponds to a tilt angle θ_T of one of the mirrors in an ordinary Michelson interferometer. The third, shown in Fig. 2(c), is a translation of one line relative to the other in a plane normal to the $\hat{x}$ axis. We call the normal displacement I between the two lines the lateral shear. It causes effects analogous to those seen in an ordinary Michelson interferometer when the light is not normally incident on the plane reflectors. A similar shear arises in Michelson interferometers equipped with corner cube reflectors. The OTF of a component in the output beam can be measured by changing the lateral shear. The fourth, shown in Fig. 2(d), is a rotation of one line relative to the other in a plane perpendicular to the $\hat{x}$ axis. We call this angle θ_S the rotary shear.

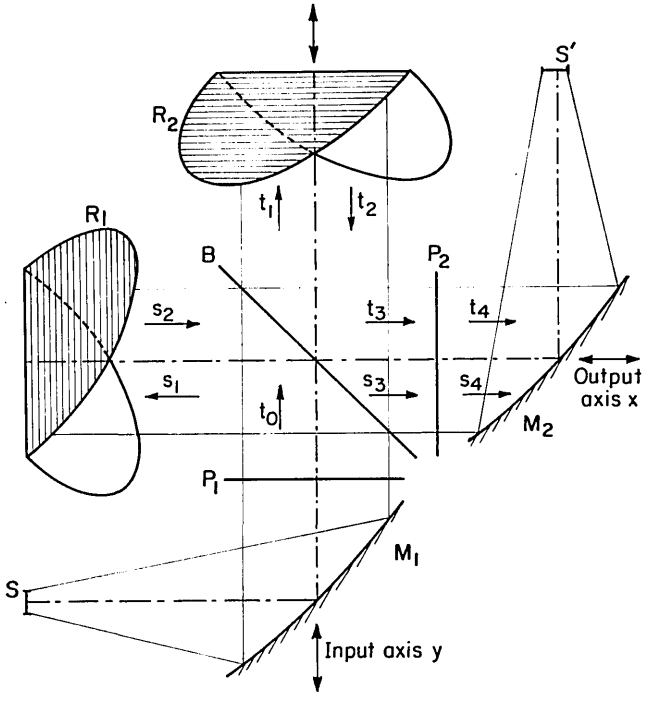

540

Fig. 1. A version of the MPI used for laboratory far-ir Fourier spectroscopy. The important features are the Hg arc source S, the paraboloidal collimating mirror M_1, the input grid polarizer P_1, the grid beam splitter B, the fixed roof mirror R_1, the moving roof mirror R_2, the output grid polarizer P_2, the focusing paraboloid M_2, and the entrance aperture S' to the light pipe leading to the detector. The normal to the plane of the polarizer P_2 is tilted away from the $\hat{x}$ axis so that radiation reflected from it cannot reach S'. For some applications it is useful to tilt P_1 and P_2 through ~45° so as to provide access to the two possible input beams and the two output beams. The wires in the beam splitter are in the $\hat{x}$-$\hat{y}$ plane so that diffracted radiation will not remain in the plane of the interferometer. The polarizer P_2 is rotated to modulate the signal. (It is actually located near S' in our instrument.) The lower case letters s_i and t_i refer to various beams in the interferometer.

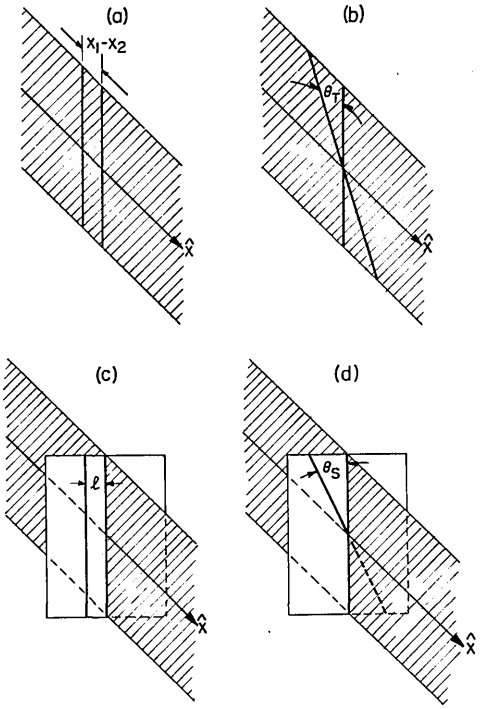

XBL775-5541

Fig. 2. Path difference (a) produces a translation of the image along the $\hat{x}$ axis, tilt (b) produces a rotation in a plane containing the $\hat{x}$ axis, lateral shear (c) is a translation perpendicular to the $\hat{x}$ axis, and rotary shear (d) is a rotation about the $\hat{x}$ axis.

In a later section we will discuss the effect on the interferogram of deviations of the optical components from the ideal configuration. We will show that all first-order effects of misalignment vanish if both roof mirrors have the same dihedral angle which is close to 90° ($\theta_{R1} = \theta_{R2} \simeq \pi/2$) if there is no tilt, lateral shear, or rotary shear, and if the angle of the input polarizer P_1 is adjusted to balance the intensity in the two beams.

II. Fourier Spectroscopy

We now discuss the use of the MPI for Fourier spectroscopy. For simplicity we begin by examining the output of the interferometer if an unpolarized plane wave of wavenumber $\sigma = 1/\lambda$ is incident on P_1 along the $\hat{y}$ axis. In the Appendix we compute the electric field throughout the interferometer. If the electric field has amplitude E_o after passing through P_1, after P_2 (which is rotating at frequency ω) the electric field is given by the real part of

$$\mathbf{E}_{\text{out}} = E_o(0, \sin\omega t, \cos\omega t)\,\{[\cos(\omega t)/\sqrt{2}]\exp(-4\pi i\sigma x_1) + [\sin(\omega t)/\sqrt{2}]\exp(-4\pi i\sigma x_2)\}\exp[2\pi i\sigma(x - ct)]. \quad (1)$$

Hence, the fraction of the power in the incident unpolarized quasi-monochromatic wave which reaches the detector is

$$\frac{I_{\text{out}}}{I_{\text{in}}} = \frac{|\mathbf{E}_{\text{out}}|^2}{2E_o^2} = \frac{1}{4}[1 + \sin(2\omega t)\cos 4\pi\sigma(x_1 - x_2)]. \quad (2)$$

If we use a lock-in amplifier to demodulate the output power at frequency 2ω, the output signal will be

$$F_{\mathrm{MPI}}(x_1 - x_2) = \frac{1}{4}\cos 4\pi\sigma(x_1 - x_2). \tag{3}$$

An interferogram is obtained by changing either x_1 or x_2 and measuring $F_{\mathrm{MPI}}(x_1 - x_2)$ as a function of position.

We can compare this result with that for an ordinary Michelson interferometer with an ideal dielectric beam splitter which reflects half the power and transmits half the power in an incident plane wave of wavenumber σ. Let us suppose that this interferometer uses a sine wave chopper which transmits light according to $I_{\mathrm{trans}} = I_{\mathrm{incident}}(1 + \sin 2\omega t)/2$. Then the fraction of the power from the source which reaches the detector is

$$\frac{I_{\mathrm{out}}}{I_{\mathrm{in}}} = \frac{1}{4}(1 + \sin 2\omega t)\{1 + \cos[4\pi\sigma(x_1 - x_2)]\}. \tag{4}$$

If we demodulate the output power of the ordinary Michelson interferometer with a lock-in amplifier at frequency 2ω, the output signal will be

$$F_{\mathrm{MI}}(x_1 - x_2) = \frac{1}{4}\{1 + \cos[4\pi\sigma(x_1 - x_2)]\}. \tag{5}$$

We see that the only difference between these two idealized interferometers when used in the chopped mode is that the ordinary Michelson interferometer produces an extra constant signal proportional to the source intensity which is independent of path difference. When used with an unpolarized source, the amplitude of the modulated portion of the interferogram is the same for the two instruments.

The beam-splitter efficiency of a practical MPI is essentially ideal for wavelengths longer than the cutoff of the grid polarizers. The MPI is superior in this regard to other far ir interferometers such as the ordinary Michelson interferometer with Mylar beam splitters or the lamellar grating interferometer.[11]

It is well known that the constant term in the interferogram of an ordinary Michelson interferometer used in the chopped mode is very troublesome in practice. Because of it, fluctuations in the source intensity or the detector sensitivity appear as spurious Fourier components in the interferogram and cause errors in the measured spectrum. The absence of this term is an important advantage of the MPI in the spectroscopic application. A constant term does arise in the MPI if the beam splitter does not polarize completely over the spectral range detected. The theory of this effect is given in a later section. Since grid polarizers are available which are very efficient over a wide range of ir wavelengths,[12] the constant term which arises from imperfect polarization is not very important at far ir wavelengths.

III. Misalignments and Imperfections

To begin our consideration of the real interferometer we discuss how the actual displacements of the optical components from the ideal configuration are related to the tilt, lateral shear, and rotary shear discussed in Sec. I. We do this using the vector relations between the directions of the incident and reflected beams given in the Appendix. Using the labels for the direction of propagation of the various beams given in Fig. 1 we find that

$$\left.\begin{aligned}
\hat{s}_1 &= \hat{t}_0 - 2(\hat{t}_0 \cdot \hat{n}_B)\hat{n}_B, \\
\hat{s}_2 &= -\hat{s}_1 + 2(\hat{s}_1 \cdot \hat{n}_{R1})\hat{n}_{R1}, \\
\hat{s}_3 &= \hat{s}_2, \\
\hat{t}_1 &= \hat{t}_0, \\
\hat{t}_2 &= -\hat{t}_1 + 2(\hat{t}_1 \cdot \hat{n}_{R2})\hat{n}_{R2}, \\
\hat{t}_3 &= \hat{t}_2 - 2(\hat{t}_2 \cdot \hat{n}_B)\hat{n}_B.
\end{aligned}\right\} \tag{6}$$

The difference in direction between the two output beams from the interferometer resulting from a given input direction $\hat{t}_0$ is

$$\begin{aligned}
\hat{s}_3 - \hat{t}_3 = 2[&(\hat{t}_0 \cdot \hat{n}_{R1})\hat{n}_{R1} - 2(\hat{t}_0 \cdot \hat{n}_B)(\hat{n}_B \cdot \hat{n}_{R1})\hat{n}_{R1} \\
&- (\hat{t}_0 \cdot \hat{n}_{R2})\hat{n}_{R2} + 2(\hat{t}_0 \cdot \hat{n}_{R2})(\hat{n}_{R2} \cdot \hat{n}_B)\hat{n}_B].
\end{aligned} \tag{7}$$

This is an exact result. We linearize it in terms of deviations of $\hat{t}_0$, $\hat{n}_B$, $\hat{n}_{R1}$, and $\hat{n}_{R2}$ from the values given in the introduction for the perfectly aligned instrument. We let

$$\left.\begin{aligned}
\Delta\mathbf{t}_0 &= a_t\left(\frac{1}{\sqrt{2}}, 0, \frac{1}{\sqrt{2}}\right) + b_t\left(-\frac{1}{\sqrt{2}}, 0, \frac{1}{\sqrt{2}}\right) \\
\Delta\mathbf{n}_B &= a_B\left(-\frac{1}{\sqrt{3}}, \frac{1}{\sqrt{3}}, -\frac{1}{\sqrt{3}}\right) + b_B\left(\frac{1}{\sqrt{6}}, -\frac{1}{\sqrt{6}}, -\frac{2}{\sqrt{6}}\right) \\
\Delta\mathbf{n}_{R1} &= a_{R1}(1,0,0) + b_{R1}\left(0, \frac{1}{\sqrt{2}}, \frac{1}{\sqrt{2}}\right) \\
\Delta\mathbf{n}_{R2} &= a_{R2}(0,-1,0) + b_{R2}\left(\frac{1}{\sqrt{2}}, 0, -\frac{1}{\sqrt{2}}\right).
\end{aligned}\right\} \tag{8}$$

In terms of these eight angular deviations Eq. (7) becomes, to first order,

$$\hat{s}_3 - \hat{t}_3 = (2\sqrt{3}a_B - 2a_{R1} + 2a_{R2})\hat{n}_{R1}. \tag{9}$$

We see that the angle of tilt of the interferometer is $\theta_T = \sqrt{3}a_B - a_{R1} + a_{R2}$. Further inspection shows that b_B introduces a lateral shear and that the angle of rotary shear is $\theta_S = b_{R1} - b_{R2}$. There is no first-order effect from changes in $\hat{t}_0$.

Since the detected interference can only occur between spectral components separated in frequency by less than the bandwidth of the detection system, we may consider separately each spectral component σ in calculating the interference between the two beams. For each misalignment we will calculate the factor $Q(q_i,\sigma)$ by which the interference modulation in the interferogram resulting from light of wavenumber σ is reduced through the misalignment parameter q_i. To calculate Q we will use the concept of two beam coherence[13] which is developed more extensively in the companion paper.[5] The total electric field is the superposition of the field from each beam. Let $E_s(\mathbf{x},\sigma)$ and $E_t(\mathbf{x},\sigma)$ be the time Fourier component of the electric field at the point $\mathbf{x}$ in the beams x and t, respectively. We proceed by analogy to the well known theory of partial coherence between two points in a single beam[14] and define a two-beam partial coherence function at wavenumber σ by

$$W_{st}(\mathbf{x}_1,\mathbf{x}_2,\sigma) = [E_s(\mathbf{x}_1,\sigma)E_t^*(\mathbf{x}_2,\sigma)]/[|E_s(\mathbf{x}_1,\sigma)||E_t(\mathbf{x}_2,\sigma)|]. \tag{10}$$

This quantity satisfies the condition $|W_{st}(\mathbf{x}_1,\mathbf{x}_2,\sigma)| \leq 1$. The real part is directly related to how much the light from the two beams of a given wavenumber will interfere at a given point. If $W_{st}(\mathbf{x},\mathbf{x},\sigma) = 1$, the two beams interfere constructively at $\mathbf{x}$. If $W_{st}(\mathbf{x},\mathbf{x},\sigma) = -1$, they interfere destructively. If $\mathrm{Re}\,W_{st}(\mathbf{x},\mathbf{x},\sigma) = 0$ there is no interference at $\mathbf{x}$. For example, if all the misalignment parameters are zero and there is zero path difference, $E_s(\mathbf{x},\sigma) = E_t(\mathbf{x},\sigma)$ for each point $\mathbf{x}$ on the entrance to the detector and $W_{st}(\mathbf{x},\mathbf{x},\sigma) = 1$.

Many of the effects which occur in the MPI are well known from the ordinary Michelson interferometer and so will not be analyzed in detail.[15] Among these are effects due to lack of flatness of the mirrors, the apparent shift in wavenumber and loss of modulation at large path difference caused by the finite throughput of the system, effects due to errors in the translation stage which produces the path difference, etc. The effect of aberrations in the input collimating optics may be analyzed using the ordinary theory of partial coherence since they occur before the two beams are divided.[5] It may be shown that input collimation aberrations are equivalent to using a source with a different intensity distribution and coherence than the actual source.

IV. Tilt

If we introduce a tilt θ_T into the interferometer, the image of one beam is shifted through a displacement $\mathbf{d}$ relative to the other, where $|\mathbf{d}| = 2\theta_T f_2$, and f_2 is the focal length of M_2. Then $E_s(\mathbf{x},\sigma) = E_t(\mathbf{x} + \mathbf{d},\sigma)$ so $W_{st}(\mathbf{x},\mathbf{x},\sigma)$ is equal to the ordinary quasi-monochromatic partial coherence[14] between the two points $\mathbf{x}$ and $\mathbf{x} + \mathbf{d}$ in one of the beams. If we assume that the aperture stop is located after the interferometer and that both the aperture stop and field stop are uniformly illuminated by both beams (even when shifted), the measured interference is found from the partial coherence of the light in a single beam between two points separated by $\mathbf{d}$. If the aperture stop is circular and of radius r_0 this quantity is calculated using the van Cittert-Zernike theorem[16] to be $W(\mathbf{x},\mathbf{x} + \mathbf{d}, \sigma) = 2J_1(u)/u$, where J_1 is Bessel's function of order unity and where $u = 2\pi\sigma r_0|\mathbf{d}|/f_2$. Hence the factor Q_T by which the tilt reduces the modulation of the interferogram corresponding to wavenumber σ is

$$Q_T = 2J_1(u)/u, \tag{11}$$

where $u = 4\pi\sigma r_0\theta_T$. This is the standard result for tilt in an ordinary Michelson interferometer.[15]

V. Lateral Shear

We next discuss the effects produced when a lateral shear $\mathbf{l}$ is introduced between the two beams. There are then two limiting cases of interest. These arise upon comparing the lateral distance over which light incident on the output collimating optics is spatially coherent, with the distance over which the optics preserve an incident wavefront to an accuracy of $\lambda/4$. If the first distance is much smaller than the second, the light in a single beam incident on M_2 can be considered spatially incoherent. In a companion paper[5] we show that in this case the two-beam coherence at a given point $\mathbf{x}$ in the image plane $W_{st}(\mathbf{x},\mathbf{x},\sigma)$ is equal to $\Lambda(\mathbf{K})$, the optical transfer function of M_2, where $\mathbf{K} = 2\sigma\mathbf{l}/f_2$. Here $\Lambda(\mathbf{K})$ is defined as the ratio of the Fourier component of the intensity in the image plane with spatial frequency $\mathbf{K}$ to the corresponding Fourier component in the object plane. The OTF $\Lambda(\mathbf{K})$ is normalized such that $\Lambda(\mathbf{0}) = 1$. Because $\Lambda(\mathbf{K})$ is complex, both the phase and the amplitude of a given Fourier component of the interferogram will change when shear is introduced between the two beams. The phase change causes what is commonly called a chirping of the interferogram.

In the other limiting case the output collimating optics are rough over a typical region of coherence of the light beam. For instance, the equivalent of ground glass could be put in the output beam. In this case the interference we are measuring is localized in the plane of surface roughness and not at the entrance to the detector. In the companion paper[5] it is shown that in this case the two-beam coherence at a point on the entrance plane to the detector is just the ordinary partial coherence between two points separated by $2\mathbf{l}$ in the plane of surface roughness. The partial coherence between two points in this plane is calculated from the van Cittert-Zernike theorem to be $W(\mathbf{x},\mathbf{x} + 2\mathbf{l}, \sigma) = 2J_1(x)/x$, where $x = 4\pi\sigma r_1|\mathbf{l}|/f_1$. Here r_1 is the radius of the source, and f_1 is the focal length of M_1. Hence, in this limit, $W_{st}(\mathbf{x},\mathbf{x},\sigma) = 2J_1(u)/u$, where $u = 4\pi\sigma r_1|\mathbf{l}|/f_1$.

The general case in which there is both partially coherent light and imperfect optics is shown in the companion paper[5] to be a convolution of these two limiting cases. For the case in which both beams have uniform intensity across the aperture of the output collimating optics, this result[17] can be summarized by writing the modulation amplitude Q_{LS} as $|M(\mathbf{l},\sigma)|/|M(\mathbf{0},\sigma)|$, where

$$M(\mathbf{l},\sigma) = \int W[\mathbf{x}, \mathbf{x} + 2(\mathbf{l} - \mathbf{r}), \sigma]\Lambda(2\sigma\mathbf{r}/f_2,\sigma)d^2r. \tag{12}$$

The phase shift of the modulation of the interferogram is given by the phase of the complex number $M(\mathbf{l},\sigma)/M(\mathbf{0},\sigma)$. Our method of measuring the OTF follows from this relationship. It is useful to observe that since $Q_{LS} = 1$ for $\mathbf{l} = 0$ irrespective of the partial coherence in a single beam, then for small lateral shear, Q_{LS} is bounded below by both of the extreme conditions

$$\begin{aligned} Q_{LS} &> |\Lambda(\mathbf{K})|, \quad \text{where } \mathbf{K} = 2\sigma\mathbf{l}/f_2, \\ Q_{LS} &> 2J_1(u)/u, \quad \text{where } u = 4\pi\sigma r_1|\mathbf{l}|/f_1. \end{aligned} \tag{13}$$

VI. Rotary Shear

When rotary shear is introduced into the interferometer there are two distinct effects. One of these has to do with the fact that rotary shear in the MPI rotates the relative polarization of the two beams. The beam splitter cannot then be in a proper orientation to let both beams recombine completely. If only one roof mirror is rotated the effect is proportional to $\cos 2\theta_S$. Of course there will be no loss of interference if both roof mirrors and the projection of $\hat{u}_B$ and $\hat{u}_{P1}$ on a plane

perpendicular to the $\hat{y}$ axis are all rotated together through the same angle. A second effect is almost the same as lateral shear, but increases with distance from the $\hat{x}$ axis. The two limiting cases of spatially incoherent light in the output beam or very rough optics that were described in the case of lateral shear also apply to this effect.

If the imaging system is free of imperfections, one image of the source will rotate relative to the other on the entrance to the detector. Again assuming that the beams are spatially uniform, the interference at a given point on the entrance to the detector is the partial coherence of the light in a single beam between that point and a point rotated through $2\theta_S$ about the center of the image. In this case the factor Q_{RS} can be found by averaging $W_{st}(\mathbf{x},\mathbf{x},\sigma)$ over the entrance to the detector. We find

$$Q_{RS} = \cos(2\theta_S)[1 - J_0(2x)]/x^2, \quad \text{where } x = 2\pi\theta_S\sigma r_2 r_0/f_2. \quad (14)$$

If there are imperfections of the collimating optics, there is an additional small loss of modulation due to relative distortion of the images produced by the rotation of one beam relative to the other.

The other limiting case occurs if the imaging system is relatively rough. The two-beam coherence at a single point is then found in the same way, except that the two points at which the partial coherence is to be evaluated are in the plane of roughness—not at the entrance to the detector. In this case

$$Q_{RS} = \cos(2\theta_S)[1 - J_0(2x)]/x^2, \quad \text{where } x = 2\pi\theta_S\sigma r_1 r_0/f_1. \quad (15)$$

In our interferometer $r_1 = r_2$ and $f_1 = f_2$ so these two cases give the same result. Since rotary shear separates the two images by a distance $\lesssim 2\theta_S r_2$, it is a much smaller effect than that of angular tilt which separates the images by $2\theta_T f_2$.

VII. Dihedral Angle

If the dihedral angle of a roof mirror is not 90°, an incident beam of light emerges in two directions. In general, the MPI with nonorthogonal roof mirrors will have four output beams rather than two. The angular difference in direction between the two beams of a single roof mirror for small $\Delta\theta_R = \theta_R - \pi/2$ is given by Eq. (A4) in the Appendix. We find to first order in $\Delta\theta_{R1}$ and $\Delta\theta_{R2}$ that the corresponding change in direction of the output beam is

$$\Delta s_3 = \pm 2\Delta\theta_{R1}(\hat{s}_3 \cdot \hat{n}_{R1}), \qquad \Delta t_3 = \pm 2\Delta\theta_{R2}(\hat{t}_3 \cdot \hat{n}_{R1}). \quad (16)$$

Light passing through points separated by more than a coherence length from a point $\mathbf{x}$ in a given beam does not interfere (when the two beams are brought together) with the light in the other beam passing through the point corresponding to $\mathbf{x}$. This result is derived in the companion paper.[5] If the radius of coherence $r_c = f_1/\sigma r_1$ of the light inside the MPI is much smaller than the beam radius r_o, the light from one half of one roof mirror only interferes with light from the corresponding half of the other roof mirror. We see that if a dihedral angle is not 90°, the MPI is effectively separated into two interferometers. If both dihedral angles are the same, both interferometers will be aligned. The effect of an error in dihedral angle is the same as tilt. If we let $\theta_D = \Delta\theta_{R1} - \Delta\theta_{R2}$, the loss of modulation with respect to pathlength is

$$Q_D = 2J_1(v)/v, \quad (17)$$

where $v = 2\pi\sigma r_o\theta_D$.

VIII. Beam Splitter and Polarizers

We now consider the effect of setting the input polarizer at an incorrect angle. This will change the fraction of the intensity in one beam relative to the other. If we let θ_P be the angle by which the projection of $\hat{u}_1$ on a plane normal to the $\hat{y}$ axis is rotated with respect to $\hat{u}_1$ in the ideal instrument, Eq. (1) becomes

$$\mathbf{E}_{\text{out}} = E_o(0, \sin\omega t, \cos\omega t)\left[\cos\left(\theta_P + \frac{\pi}{4}\right)\cos\omega t\,\exp(-4\pi i\sigma x_1) + \sin\left(\theta_P + \frac{\pi}{4}\right)\sin\omega t\,\exp(-4\pi i\sigma x_2)\right]\exp[2\pi i\sigma(x - ct)]. \quad (18)$$

Hence, the fraction of light of wavenumber σ reaching the detector is

$$\frac{I_{\text{out}}}{I_{\text{in}}} = \frac{1}{4}[1 - (\cos 2\omega t)\sin 2\theta_P + (\sin 2\omega t)(\cos 2\theta_P)\cos 4\pi\sigma(x_1 - x_2)]. \quad (19)$$

An incorrect polarizer angle reduces the detected modulation on the interferogram by $\cos 2\theta_P$ and introduces a constant signal 90° out of (lock-in) phase from the interferogram, whose amplitude is proportional to $\sin 2\theta_P$.

Next we examine the effects due to incomplete polarization by the beam splitter. Let R_a and R_b be the complex reflection coefficients for polarization states with electric field perpendicular to the wires and the orthogonal polarization state, respectively. They describe the amplitude and phase of the light reflected from the wires with respect to that from a perfectly conducting metal mirror in the plane of the wires. Let T_a and T_b be the analogous coefficients with respect to transmission in the absence of the wires.

If we use the vector relations given in the Appendix to follow the polarization state of the electric field through the beams in Fig. 1, we find

$$\mathbf{E}_{s4} = \frac{E_o}{\sqrt{2}}(0, \sin\omega t, \cos\omega t)\cdot(R_b T_a \sin\omega t + R_a T_b \cos\omega t)\cdot\exp[2\pi i\sigma(\hat{x}\cdot\mathbf{r} - ct - 2x_1)].$$

$$\mathbf{E}_{t4} = \frac{E_o}{\sqrt{2}}(0, \sin\omega t, \cos\omega t)\cdot(R_a T_b \sin\omega t + R_b T_a \cos\omega t)\cdot\exp[2\pi i\sigma(\hat{x}\cdot\mathbf{r} - ct - 2x_2)]. \quad (20)$$

Here we have assumed that the angle of the input polarizer is adjusted to balance the intensity of light in the two beams. The ratio of output intensity to input intensity from an unpolarized source is $I_{\text{out}}/I_{\text{in}} = \mathbf{E}_{\text{out}}\cdot\mathbf{E}_{\text{out}}^*/2E_o^2$. Hence

$$\frac{I_{out}}{I_{in}} = \frac{1}{4}\{|R_b|^2|T_a|^2 + |R_a|^2|T_b|^2 + 2\,\mathrm{Re}(R_aR_b{}^*T_a{}^*T_b)\cos 4\pi\sigma(x_1 - x_2) + \sin 2\omega t[2\,\mathrm{Re}(R_aR_b{}^*T_a{}^*T_b) + (|R_a|^2|T_b|^2 + |R_b|^2|T_a|^2) \cdot \cos 4\pi\sigma(x_1 - x_2)] + 2\cos(2\omega t)\,\mathrm{Im}(R_aR_b{}^*T_a{}^*T_b)\sin 4\pi\sigma(x_1 - x_2)\} \quad (21)$$

For a perfect beam splitter $|R_a| = |T_b| = 0$ and $|R_b| = |T_a| = 1$. We see that a real beam splitter has efficiency $\epsilon = |R_a|^2|T_b|^2 + |R_b|^2|T_a|^2$ and that there is an offset contribution $n^{(r)} = 2\,\mathrm{Re}(R_aR_b{}^*T_a{}^*T_b)$ to the symmetric interferogram demodulated by the lock-in amplifier. If we change the lock-in phase by 90°, an antisymmetric interferogram will appear. The contribution by wavenumber σ to this interferogram is $n^{(i)} = 2\,\mathrm{Im}(R_aR_b{}^*T_a{}^*T_b)$.

Along with incomplete polarization by the beam splitter we may also examine the effects due to incomplete polarization by the input and output polarizers. If the input polarizer P_1 is removed, the output intensity is found to be

$$\frac{I_{out}}{I_{in}} = \frac{1}{2}\epsilon + \frac{1}{2}n^{(r)}\cos 4\pi\sigma(x_1 - x_2) + \cos 2\omega t\left[\frac{1}{2}n^{(i)} \cdot \sin 4\pi\sigma(x_1 - x_2)\right]. \quad (22)$$

Hence, if P_1 transmits a fraction χ_1 of polarized light and a fraction $1 - \chi_1$ of unpolarized light,

$$\frac{I_{out}}{I_{in}} = \frac{1}{4}\{\epsilon + n^{(r)}\cos 4\pi\sigma(x_1 - x_2) + \chi_1(\sin 2\omega t) \cdot [n^{(r)} + \epsilon\cos 4\pi\sigma(x_1 - x_2)] + n^{(i)}\cos 2\omega t\,\sin 4\pi\sigma(x_1 - x_2)\}. \quad (23)$$

We see that the demodulated signal from the lock-in amplifier depends linearly on χ_1. Evidently if the output polarizer transmits a fraction χ_2 of polarized light and a fraction $1 - \chi_2$ of unpolarized light, the demodulated signal will depend linearly on χ_2. Also, if polarizer P_1 attenuates a polarized light beam in the state that should be transmitted by a factor A_1 the output is reduced by the same factor and similarly for attenuation by a factor A_2 by polarizer P_2. Hence the demodulated signal is reduced by a factor

$$Q_P = \epsilon\chi_1\chi_2A_1A_2\cos 2\theta_P. \quad (24)$$

We also observe that if beam t is blocked,

$$\frac{I_{out}}{I_{in}} = \frac{1}{8}[\epsilon + n^{(r)}\sin 2\omega t - (|R_a|^2|T_b|^2 - |R_b|^2|T_a|^2)\cos 2\omega t]. \quad (25)$$

Also, if beam s is blocked,

$$\frac{I_{out}}{I_{in}} = \frac{1}{8}[\epsilon + n^{(r)}\sin 2\omega t + (|R_a|^2|T_b|^2 - |R_b|^2|T_a|^2)\cos 2\omega t]. \quad (26)$$

As will be discussed in the next section, these results make it possible to measure conveniently the alignment of the MPI.

Thus far we have not discussed the effects of inhomogeneity in the wire separation in the beam splitter. This will cause the reflection and transmission coefficients to be position dependent. Short wavelength Fourier components of the inhomogeneity will diffract energy away from the detector. Long wavelength Fourier components, especially those which diffract through angles $\simeq r_2/f_2$, change the optical path traveled by part of the light reaching the detector and thus reduce the detected interference. In the presence of a lateral shear, long wavelength fluctuations in the wire separation are equivalent to aberrations in the output collimating optics. The MPI can be used for OTF measurements only if the beam splitter quality is better than that of the output optics to be measured.

IX. Alignment

The MPI should be constructed so that there are orthogonal adjustments for tilt, lateral shear, rotary shear, dihedral angle, and the angle of the input polarizer. If it is desired to use the instrument for OTF measurements as well as for Fourier transform spectroscopy, the lateral shear adjustment must be calibrated.

The interferometer is aligned by the following procedure.

(1) We use cross-hairs to establish a pair of intersecting optic axes.

(2) We position the beam splitter B so that a ray on the first optic axis is reflected onto the second. To do this we replace the roof mirrors with two flat mirrors so that a He–Ne laser beam traveling along each axis is reflected back into the laser. We then align B so that the two output laser beams reflected off the surface of a glass plate pressed against the wires coincide in the far field.

(3) We use a well collimated parallel beam of light directed along each optic axis to adjust each paraboloid so that its axis is parallel to the optic axis and the beam is focused on the center of the input or output aperture.

(4) We visually align each roof mirror before installation so that the dihedral angle is 90°. After the interferometer is operating, it is necessary to adjust precisely one of the dihedral angles to peak up the signal detected at zero path difference.

(5) We set the tilt and shear to zero visually by looking into the interferometer with the collimating optics removed as discussed in Sec. I. These adjustments should be improved upon after the interferometer is operating by peaking up the detected zero path difference signal. Although the tilt and lateral shear are orthogonal at the virtual positions of the roof mirrors, they are not orthogonal in their effect when the two beams reach the output collimating optics. A nonzero tilt will produce an effective lateral shear at that point. (However, a nonzero shear will not produce a tilt.)[5] For this reason, the final adjustments of tilt and shear must be done iteratively. The effect of rotary shear is orthogonal to tilt and lateral shear. It need only be adjusted once and is not included in the iteration procedure. The same is true of the dihedral angle adjustment.

(6) We adjust the phase of the lock-in amplifier to minimize the detected modulation in the interferogram.

We then adjust the angle of the input polarizer until the baseline of the residual modulation is zero. The phase of the lock-in amplifier is then changed by 90°.

In principle there should be another adjustment to rotate the wires of the beam splitter by an angle θ_W in the plane of the beam splitter. The loss of interference due to this misalignment is only proportional to $\cos 2\theta_W$ and can be made very small if the interferometer is constructed carefully.

When the alignment procedure is finished it is desirable to measure how well the interferometer is aligned. We now discuss how this can be done. If the intensity of the light modulated at frequency 2ω by the rotating polarizer is I_{s+t} with both beams present, I_s with the beam t blocked, and I_t with the beam s blocked, from Eqs. (21), (25), and (26), we find

$$\begin{aligned} I_{s+t} &= \frac{1}{4}\{[n^{(r)} + \epsilon\,\mathrm{Re}W_{st}(\sigma)]^2 + [n^{(i)}\,\mathrm{Im}W_{st}(\sigma)]^2\}^{1/2}, \\ I_s &= \frac{1}{8}[(\epsilon - 2|R_b|^2|T_a|^2)^2 + n^{(r)2}]^{1/2}, \\ I_t &= \frac{1}{8}[(\epsilon - 2|R_b|^2|T_a|^2)^2 + n^{(r)2}]^{1/2}. \end{aligned} \tag{27}$$

Here $W_{st}(\sigma)$ is the two-beam coherence $W_{st}(\mathbf{x},\mathbf{x},\sigma)$ averaged over the entrance to the detector. We recall that if $W_{st}(\sigma) = 1$, the interferometer is perfectly aligned. If $W_{st}(\sigma) = 0$, the two beams do not interfere. If we restrict the range of experimental frequencies to those for which the beam splitter is an effective polarizer, the quantities $n^{(r)}$, $n^{(i)}$, and $|R_b|^2|T_a|^2$ are all small. Then for a single wavevector σ, $I_{s+t}/2(I_sI_t)^{1/2} = \mathrm{Re}W_{st}(\sigma)$. For a spectral distribution $B(\sigma)$,

$$I_{st}/2(I_sI_t)^{1/2} = \int_{\sigma=0}^{\infty} B(\sigma)\,\mathrm{Re}W_{st}(\sigma)d\sigma \Big/ \int_{\sigma=0}^{\infty} B(\sigma)d\sigma. \tag{28}$$

This quantity gives an easily measured test of the alignment of the interferometer. Measurements with our laboratory interferometer have given $I_{st}/2(I_sI_t)^{1/2} = 0.984 \pm 0.005$ and $n^{(r)} < 0.005$ for a spectral band limited to $\sigma \lesssim 50\ \mathrm{cm}^{-1}$ by the use of an InSb detector.

X. OTF Measurements

We now describe how the MPI may be used for OTF measurements. This is done by taking short interferograms of a broadband source for a succession of known values of lateral shear $\mathbf{l}$. (The aperture of the entrance plane of the detector must be no larger than an isoplanatic patch[18] in the image plane.) The complex amplitude $M(\mathbf{l},\sigma)$ for each wavenumber in the Fourier transform is then computed. From Eq. (12) we see that $M(\mathbf{l},\sigma)$ is a convolution of the desired OTF with the partial coherence $W(\mathbf{x},\mathbf{x},\sigma)$ in a single beam of light incident on the output collimating optics. If $W(\mathbf{x},\mathbf{x},\sigma)$ can be approximated as a δ function centered at $\mathbf{x}$ in Eq. (12), the OTF $\Lambda(\mathbf{K},\sigma) = M(f_2\,\mathbf{K}/2\sigma, \sigma)/M(\mathbf{0},\sigma)$. This condition is met if $M(\mathbf{l},\sigma)$ varies very little as $\mathbf{l}$ takes values $\mathbf{l} = \mathbf{l}_o + \mathbf{r}$, where $|\mathbf{r}| < r_c = f_1/\sigma r_1$.

When this condition is not met one may calculate $\Lambda(\mathbf{K},\sigma)$ only if both $M(\mathbf{l},\sigma)$ and $W(\mathbf{x}, \mathbf{x} + 2\mathbf{l}, \sigma)$ are known for all $\mathbf{l}$. The required procedure is discussed in the companion paper.[5] Since the MPI only allows $\mathbf{l}$ to vary in one direction, one must rotate the output collimating optics to make a complete measurement of the OTF of a system which lacks axial symmetry.

XI. Conclusion

In conclusion, the MPI is a very efficient instrument for Fourier transform spectroscopy in the far ir. The absence of a dc offset of the interferogram makes accurate spectroscopy in a fluctuating environment much more convenient than with the conventional Michelson interferometer. It may also be used to measure the OTF of far ir optics. The systematic alignment of the interferometer is found to be only slightly more complicated than for an ordinary Michelson interferometer. We recommend its use to other workers in the field.

We gratefully acknowledge helpful discussions with C. D. Andriesse and D. P. Woody.

This work was supported by the U. S. Energy Research and Development Administration.

Appendix

We first discuss the vector relations between the direction and polarization of the incident and reflected beams for a plane mirror, a perfect roof mirror, and an imperfect roof mirror with a dihedral angle unequal to 90°.

For a flat perfectly conducting mirror with unit vector $\hat{n}_m$ normal to the surface

$$\mathbf{k}_o = \mathbf{k}_i - 2(\mathbf{k}_i \cdot \hat{n}_m)\hat{n}_m; \qquad \mathbf{p}_o = -\mathbf{p}_i + 2(\mathbf{p}_i \cdot \hat{n}_m)\hat{n}_m. \tag{A1}$$

For a perfect roof mirror with dihedral angle $\pi/2$ and vector $\hat{n}_R$ along the line of intersection of the two mirrors,

$$\mathbf{k}_o = -\mathbf{k}_i + 2(\mathbf{k}_i \cdot \hat{n}_R)\hat{n}_R \qquad \mathbf{p}_o = -\mathbf{p}_i + 2(\mathbf{p}_i \cdot \hat{n}_R)\hat{n}_R. \tag{A2}$$

The analogous results for an imperfect roof mirror are more complicated. For a single input beam, we then have two output beams which are distinguished by the order in which the input beam reflects off the two mirrors. Let $\hat{n}_{m1}$ and $\hat{n}_{m2}$ denote the unit normal vectors to the two mirrors forming the roof mirror. Then we find

$$\begin{aligned} \mathbf{k}_{01} &= \mathbf{k}_i - 2(\mathbf{k}_i \cdot \hat{n}_{m2})\hat{n}_{m2} - 2(\mathbf{k}_i \cdot \hat{n}_{m1})\hat{n}_{m1} \\ &\quad + 4(\hat{n}_{m1} \cdot \hat{n}_{m2})(\mathbf{k}_i \cdot \hat{n}_{m2})\hat{n}_{m1}, \\ \mathbf{p}_{01} &= \mathbf{p}_i - 2(\mathbf{p}_i \cdot \hat{n}_{m2})\hat{n}_{m2} - 2(\mathbf{p}_i \cdot \hat{n}_{m1})\hat{n}_{m1} \\ &\quad + 4(\hat{n}_{m1} \cdot \hat{n}_{m2})(\mathbf{p}_i \cdot \hat{n}_{m2})\hat{n}_{m1}, \\ \mathbf{k}_{02} &= \mathbf{k}_i - 2(\mathbf{k}_i \cdot \hat{n}_{m1})\hat{n}_{m1} - 2(\mathbf{k}_i \cdot \hat{n}_{m2})\hat{n}_{m2} \\ &\quad + 4(\hat{n}_{m1} \cdot \hat{n}_{m2})(\mathbf{k}_i \cdot \hat{n}_{m1})\hat{n}_{m2}, \\ \mathbf{p}_{02} &= \mathbf{p}_i - 2(\mathbf{p}_i \cdot \hat{n}_{m1})\hat{n}_{m1} - 2(\mathbf{p}_i \cdot \hat{n}_{m2})\hat{n}_{m2} \\ &\quad + 4(\hat{n}_{m1} \cdot \hat{n}_{m2})(\mathbf{p}_i \cdot \hat{n}_{m1})\hat{n}_{m2}. \end{aligned} \tag{A3}$$

These results are exact. If we let $(\hat{n}_{m1} \cdot \hat{n}_{m2}) = \gamma$ and then expand the result to first order in γ, we find

$$\begin{aligned} \mathbf{k}_o^{\pm} &= -\mathbf{k}_i + 2(\mathbf{k}_i \cdot \hat{n}_R)\hat{n}_R \pm 2\gamma(\mathbf{k}_i \times \hat{n}_R), \\ \mathbf{p}_o^{\pm} &= -\mathbf{p}_i + 2(\mathbf{p}_i \cdot \hat{n}_R)\hat{n}_R \pm 2\gamma(\mathbf{p}_i \times \hat{n}_R). \end{aligned} \tag{A4}$$

We now discuss the calculation of the electric field throughout the interferometer when an unpolarized quasi-monochromatic plane wave is propagating in the $\hat{y}$ direction. We label the beams as shown in Fig. 1. The direction of the electric field in each beam is most easily found by using the vector relationships between a beam incident on an optical component and the beam reflected from it as derived above. Half of the power is transmitted by P_1, and the beam t_o is completely polarized. We trace the beam through the interferometer starting with beam t_o for the ideal instrument. We find

$$\mathbf{E}_{to} = E_o\left(-\frac{1}{\sqrt{2}}, 0, \frac{1}{\sqrt{2}}\right)\exp[2\pi i\sigma(\hat{y}\cdot\mathbf{r} - ct)],$$

$$\mathbf{E}_{s1} = E_o\left(0, -\frac{1}{\sqrt{2}}, 0\right)\exp[2\pi i\sigma(-\hat{x}\cdot\mathbf{r} - ct)],$$

$$\mathbf{E}_{t1} = E_o\left(0,0, \frac{1}{\sqrt{2}}\right)\exp[2\pi i\sigma(\hat{y}\cdot\mathbf{r} - ct)],$$

$$\mathbf{E}_{s2} = E_o\left(0,0, \frac{1}{\sqrt{2}}\right)\exp[2\pi i\sigma(\hat{x}\cdot\mathbf{r} - ct - 2x_1)],$$

$$\mathbf{E}_{t2} = E_o\left(\frac{1}{\sqrt{2}}, 0,0\right)\exp[2\pi i\sigma(-\hat{y}\cdot\mathbf{r} - ct - 2x_2)], \qquad \text{(A5)}$$

$$\mathbf{E}_{s3} = E_o\left(0, 0, \frac{1}{\sqrt{2}}\right)\exp[2\pi i\sigma(\hat{x}\cdot\mathbf{r} - ct - 2x_1)],$$

$$\mathbf{E}_{t3} = E_o\left(0, \frac{1}{\sqrt{2}}, 0\right)\exp[2\pi i\sigma(\hat{x}\cdot\mathbf{r} - ct - 2x_2)],$$

$$\mathbf{E}_{s4} = E_o(0, \sin\omega t, \cos\omega t)\frac{\cos\omega t}{\sqrt{2}}\exp[2\pi i\sigma(\hat{x}\cdot\mathbf{r} - ct - 2x_1)],$$

$$\mathbf{E}_{t4} = E_o(0, \sin\omega t, \cos\omega t)\frac{\sin\omega t}{\sqrt{2}}\exp[2\pi i\sigma(\hat{x}\cdot\mathbf{r} - ct - 2x_2)].$$

References

1. D. H. Martin and E. Puplett, Infrared Phys. **10**, 105 (1969).
2. E. R. Peck, J. Opt. Soc. Am. **38**, 66 (1948).
3. H. H. Hopkins, Opt. Acta **2**, 23 (1955).
4. D. P. Woody, J. C. Mather, N. S. Nishioka, and P. L. Richards, Phys. Rev. Lett. **34**, 1036 (1975).
5. D. K. Lambert and P. L. Richards J. Opt. Soc. Am.(to be published).
6. M. Born and E. Wolf, *Principles of Optics* (Pergamon, New York, 1975), p. 485.
7. W. H. Steel, Opt. Acta **11**, 9 (1964).
8. E. Wolf, *Progress in Optics,* (North-Holland, Amsterdam, 1965), Vol. 5, p. 201.
9. J. C. Wyant, Appl. Opt. **14**, 1613 (1975).
10. W. H. Steel, *Interferometry* (Cambridge, London, 1967), p. 55.
11. P. L. Richards, J. Opt. Soc. Am. **54**, 1474 (1964).
12. A. E. Costley, K. H. Hursey, G. F. Neill, and J. M. Ward, J. Opt. Soc. Am. 67, 979 (1977). See also J. P. Auton, Appl. Opt. **6**, 1023 (1967).
13. H. H. Hopkins, J.Opt. Soc. Am. **47**, 508 (1957).
14. Ref. 6, p. 491.
15. A. H. Cook, *Interference of Electromagnetic Waves* (Clarendon, Oxford, 1971), p. 43.
16. Ref. 6, p. 508.
17. The real part of the quantity $M(1,\sigma)$ is proportional to the interference due to light of wavenumber σ at zero path difference. Because light of a single wavenumber causes modulation in the interferogram over a finite range of spatial frequencies, this quantity loses its precise meaning away from zero path difference. These difficulties are avoided in Ref. 5.
18. Ref. 6. p. 482.